ORIGINAL PAPER

Quantification of urban heat intensity with land use/land cover changes using Landsat satellite data over urban landscapes

Ruchi Bala[1] · Rajendra Prasad[1] · Vijay Pratap Yadav[1]

Abstract

Urban heat island (UHI) is a phenomenon which may have adverse effects on our environment and is stimulated as a result of urbanization or land cover changes. Thermal remote sensing has been found beneficial to study the effect of urbanization on UHI intensity. This paper analyses the variation in land surface temperature (LST) with land cover changes in Varanasi city of India from 1989 to 2018 using Landsat satellite images. A new index named Urban Heat Intensity Ratio Index (UHIRI) was proposed to quantify the urban heat intensity from 1989 to 2018 which was found to increase from 0.36 in year 1989 to 0.87 in year 2018. Further, contribution of each land cover towards UHI was determined using land cover contribution index (LCCI). The negative value of LCCI for water and vegetation indicates its negative contribution towards UHI, whereas positive value of LCCI for bare soil and built-ups depicted its positive contribution towards UHI. The LCCI value for urban land cover shows significant increase in 29 years, i.e. 0.49, 1.43, 3.40 and 4.37 for years 1989, 1997, 2008 and 2018, respectively. The changes in normalized LST from years 1989 to 2018 for the conversion of bare land to built-ups and vegetation to built-ups were found to be as −0.11 and 0.42, respectively. This led to conclusion that the replacement of vegetation with urban land cover has severe impact on increasing UHI intensity.

1 Introduction

In the recent past few decades, urbanization has increased as a consequence of rapid population growth which led to adverse effect on our environment. According to the population statistics provided by the United Nation, urban areas accommodate more than half of global population and also predicted the increase in this ratio in future (United Nation 2015). People's migration from rural to urban areas is the major cause for urbanization or growth in the urban sprawl at a large extent due to the increased human activity in the cities. This account for the land use and land cover (LULC) shift from natural land to impervious surface, transportation and industry modifies the thermal conduction with the environment (Shafizadeh-Moghadam et al. 2020; Kato and Yamaguchi 2005). The impervious land like buildings, roads, etc. have higher thermal capacity which captivates heat during day and releases during

night time. Consequently, higher temperatures in urban areas are detected as compared to the rural areas which can be named as the urban heat island (UHI). Thus, urbanization has a direct impact on the land surface temperature (LST) in an urban area.

Rao (1972) first mentioned about the surface urban heat island (SUHI) effect using satellite remote sensing. Thermal remote sensing data have been used for UHI or LST studies obtained from various satellite sensors. Various previous studies have demonstrated the significance of thermal infrared (TIR) data due to its accessibility at different spatial and temporal resolutions (Aniello et al. 1995; Streutker 2003; Voogt and Oke 2003; Chen et al. 2006; Tran et al. 2006; Tiangco et al. 2008; Zhang et al. 2010). UHI intensity depends on various factors like difference in LULC composition in urban and rural areas, thermal conductivities of urban surface, vegetation coverage within a city, anthropogenic discharge from human activities and built-up density (Taha 1997; Sarrat et al. 2006; Mathew et al. 2016; Zhang and Wang 2008).

Mathew et al. 2018 proposed a thermal transect method to analyse the seasonal and temporal variations in SUHI from 2003 to 2015 using MODIS thermal data in Jaipur city and found that area enclosed in each isothermal line increased from 20 to 400% indicating significant SUHI growth in

✉ Rajendra Prasad
rprasad.app@itbhu.ac.in

[1] Department of Physics, Indian Institute of Technology (BHU), Varanasi, India

12 years. Zhang and Wang (2008) discussed the spatial extent of SUHI using the relation of hot island area (HIA) with various urban characteristic in ten different cities located at same latitude and found good correlation of HIA with urban size, population density same and development area, whereas weak negative correlation with mean normalized difference vegetation index (NDVI) and water proportion was observed. Grigoraş and Uriţescu (2019) studied the effect of LULC change on SUHI from 1984 to 2016 in Bucharest, Romania, using Landsat data. The built-up and fallow land increased, whereas green land decreased by 2016, and also, the difference between the average urban and rural LST decreased representing extension in the area of UHI. Meng et al. 2018 discussed the spatial and temporal behaviour of SUHI by comparing different levels of UHI with urban main built-up area for 12 years in Beijing city of China. Li et al. (2018) developed a new method for quantifying SUHI intensity from the relation of LST with impervious surface area (ISA) using MODIS data. The ISA was regionalised using Kernel density estimation method that showed good linear relation with LST, and the slope was found effective to quantify SUHI. Keeratikasikorn and Bonafoni (2018) studied the SUHI pattern for different LULC in Bangkok using Landsat 8 data which can help for better land use planning for SUHI mitigation. Sultana and Satyanarayana (2018) studied the LULC change and LST in ten major cities of India from 2001 to 2013 using Landsat data and some ground-based measurement. Various cities showed an increase in built-up area by replacing vegetated/bare land, and some cities showed increase in built-up/bare land at the expense of agricultural land, and the hotspots increased in the built-up and bare land. Amiri et al. (2009) constructed temperature vegetation index space to study about the LULC change in urban area and its impact on urban LST in Tabriz city of Iran from 1989 to 2001 using Landsat data. Huang et al. (2019) suggested a land contribution index (LCI) to better quantify the contribution of each LULC on UHI in Wuhan city of China from using MODIS thermal data. The constructed land contributes greater to the UHI effect in summer, waterbody shows lowest contribution in spring and urban green spaces has negative contribution towards UHI effect but was not prominent during winter. The region contributing to strong UHI increased from 3.35% in 2005 to 8.56% in 2015 of the study area. Shirani-bidabadi et al. (2019) analysed different thermal levels defined from standard deviation (SD) to study the influence of urbanization on the LST from 1999 to 2016 using Landsat 7 ETM+ (Enhanced Thematic Mapper) and Landsat 8 images in Isfahan city of Iran. They proposed an index named heat island ratio that was observed in the 4 years (1999, 2006, 2013 and 2016), and UHI was significant in areas with sparse vegetation, arid land and enhanced industrialisation in the city.

The climate change in the urban environment stimulates the study on UHI which can help in the development of strategies to attenuate the negative impacts of UHI on climate. India is the second most populous country which is the major reason for increasing urbanization. Therefore, there is an acute requirement to study SUHI growth with urban expansion in Indian cities The UHI intensity depends not only on the urban LST but also on the rural land cover surrounding the urban areas. The rural land covers mainly consist of vegetation or barren land, and both shows different kind of thermal behaviour during day time which effects the determination of UHI intensity. Various previous studies discussed the combined effect of bare land and built-ups in UHI formation. Since urbanization is a result of replacing bare land or vegetative land cover with built-ups, it is important to study the effect of built-ups on UHI formation. Therefore, a new index named Urban Heat Intensity Ratio Index (UHIRI) was proposed in the present study which considers the difference of urban LST and the combined LST of rural land covers making it useful to understand the UHI intensity in cities with changing natural land cover surrounding the city. UHIRI was used to quantify the urban heat intensity from 1989 to 2018 in Varanasi city of India using Landsat satellite images. Further, contribution of each land cover towards raising or lowering of LST was determined using land cover contribution index (LCCI) for years 1989, 1997, 2008 and 2018 to analyse the variation in contribution of each land cover towards LST with change in LULC or urbanization.

2 Study area and data used

This study was performed on Varanasi city located in Indo-Gangetic planes of north India also named as Kashi with centre coordinates of 25°19′18.06″N and 82°59′14.24″E. This is one of the oldest human settlements in the world with population of almost 12 lakhs according to the Census 2011of India. This is a holy city and various ancient temples present at the city core have resulted in greater commercial development in the city. After 1980, the green spaces in the city were replaced with built-ups for the development of various commercial as well as residential building. After 1990, the boundary of the city expanded mainly due to development of new residential areas. Thus, the unplanned urban expansion has also lead to aggravated settlement patterns in urban areas with decreasing natural land covers (Jha et al. 2019). Here, the vegetated as well as barren land has been converted to built-ups which facilitate the comparative study of replacing each kind of natural land cover with urban built-ups on thermal environment. The city experiences a humid subtropical climate. Varanasi is situated between two rivers, i.e. River Varuna and River Ganga, enhancing the soil fertility for agriculture purpose. Figure 1 shows the location map of study area.
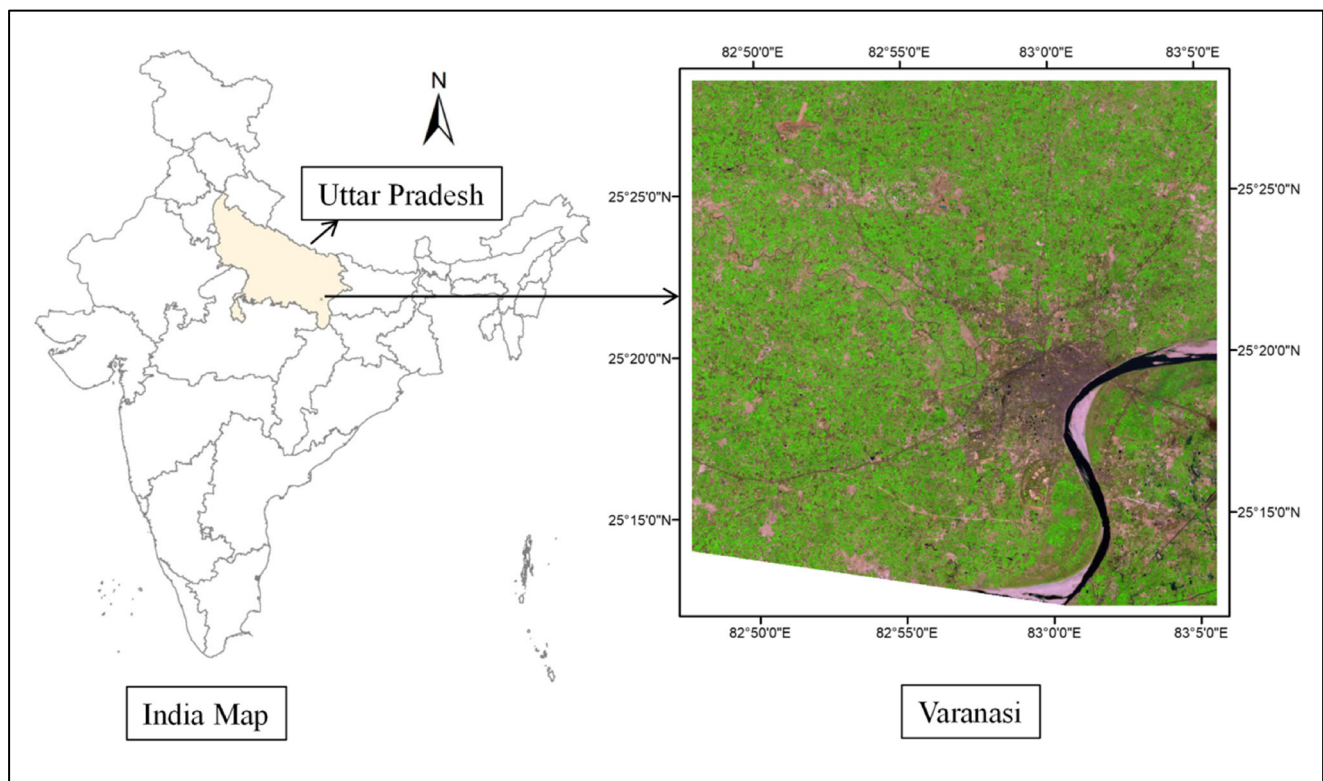
Fig. 1 Location map of the study area. The false colour composite image of Varanasi city was obtained for year 1989 from Landsat data, and the SWIR1, NIR and Green band are represented with red, green and blue colour, respectively

Landsat satellite data has been made accessible by the U.S. Geological Survey (USGS) since 1972. This provides the longest time series data at a spatial resolution of 30 m which is found most adequate for continuous monitoring of LULC changes due to urbanization. Landsat 5 TM (Thematic Mapper) and Landsat 8 OLI (Operational Land Imager) data have been used for the present study from 1989 to 2018. The data was obtained during clear sky conditions. Landsat Level 1 data products are radiometric, geometric and terrain corrected. Landsat Collection-1 Higher Level data products use AOT (aerosol optical thickness), ozone and water vapour bands obtained from MODIS data for atmospheric correction and provide the atmospheric corrected surface reflectance data that can be obtained from the US Geological survey website, i.e. https://earthexplorer.usgs.gov/. So, the reflectance bands are atmospheric corrected and can be used directly for study,

whereas thermal bands require atmospheric correction. The specification of the datasets is provided in Table 1. The images were clipped according to the defined study area.

Cirrus clouds are sometimes difficult to detect through optical bands in remote sensing data because of its transparent or semi-transparent property but can have significant impact on surface reflectance values in different optical bands. This can adversely affect the application of the time-series analysis from the satellite data (Huang et al. 2010). Qiu et al. 2020 studied the impact of cirrus clouds on blue, green, red, NIR, SWIR1 and SWIR2 bands of Landsat data and found that the presence of cirrus clouds influenced the surface reflectance of blue band most seriously, whereas the surface reflectance of SWIR2 band was least effected. The areas with dry air such as high-rise mountains and polar ice/snow regions can sometimes be identified as cirrus clouds due to its greater brightness

Table 1 Satellite data specification

Satellite	Acquisition date	Acquisition time (UTC)	Path/row	Cloud cover
Landsat 5 TM	24-02-1989	04:25	142/42	0%
Landsat 5 TM	14-02-1997	0.4:20	142/42	0%
Landsat 5 TM	29-02-2008	04:45	142/42	0%
Landsat 8 OLI	24-02-2018	04:55	142/42	0%

value. The present study was performed in region with humid subtropical climate, and the Landsat data was obtained for clear sky condition, i.e. no cloud cover present.

3 Methodology

3.1 Supervised classification and change in LULC

The false colour composite (FCC) image was obtained by combining the bands 4–3-2 from Landsat 5 TM data and bands 5–4-3 from Landsat 8 OLI data. The image was classified into four major LULC classes, i.e. water, vegetation, bare land and built-ups. The classes were defined by visual interpretation from the spectral signature of each class. Then, random forest classification algorithm was applied to obtain the classified image, and further, the classification accuracy was assessed. The total number of pixels for each LULC class was determined from each classified image and converted into percentage.

Percentage of each LULC class

$$= \frac{\text{Number of pixels occupied by each class}}{\text{Total number of pixels in a classified image}} \quad (1)$$

The post-classification method has been used to detect the change in natural land cover (bare land and vegetation) to built-ups from 1989 to 2018 (Singh 1989). The change maps obtained show spatial distribution of change in LULC with the evolution over time.

3.2 Retrieval of LST using Landsat data

Landsat data contains TIR band which is useful for determining LST image of the land surface. Band 6 from the Landsat 5 data and Band 10 from the Landsat 8 data are the TIR bands which provides thermal data in the form of digital number (DN). Therefore, estimation of LST requires various steps (Yuan and Bauer 2007). First, DN was converted into top of atmosphere radiance (TOA) (L_λ) using Eq. (2).

$$L_\lambda = M_L \times (DN) + A_L \quad (2)$$

where M_L is multiplicative and A_L is additive rescaling factor of thermal band. This TOA radiance constitutes mixed signal of energy emitted from land surface as well as atmosphere. Second, the TOA radiance was atmospheric corrected to determine the surface leaving radiance (L_T) which contains contribution only from the land surface given by Eq. (3).

$$L_T = \frac{(L_\lambda) - L_\mu - \tau \times (1-\varepsilon) \times L_d}{\tau \times \varepsilon} \quad (3)$$

where

L_μ upwelling radiance,
L_d downwelling radiance,
τ transmission and
ε emissivity.

Barsi et al. (2005) developed an atmospheric correction tool for Landsat 4–5, 7 and 8 satellite data which provides the three atmospheric parameters, i.e. L_μ, L_d and τ available at the website http://atmcorr.gsfc.nasa.gov/. The emissivity values were computed from NDVI values (Van de Griend and Owe 1993) as shown in Table 2. The NDVI image was classified into four classes based on NDVI values, and emissivity values were assigned for each class. When NDVI is less than −0.185, the land cover is mostly water. The NDVI values between −0. 185 and 0.157 resemble mainly urban or bare land, and when NDVI is greater than 0.727, it is completely vegetated land. These three regions have been assigned a specific emissivity value for each class. The NDVI values between 0.157 and 0. 727 resemble region from bare land to dense vegetation where emissivity change can be observed and can be calculated from the logarithmic equation shown in the Table 2. Further, LST image was estimated from L_T using Planck's law as shown by Eq. (4).

$$LST = \frac{K_2}{\ln\left(1 + \frac{K_1}{L_T}\right)} \quad (4)$$

where K_1 and K_2 are thermal constants obtained from the metadata file. The direct comparison of LST of different years may not be appropriate due to the seasonal and inter-annual variability. Therefore, the LST obtained was normalized to make the LST image from different years suitable for comparison.

$$NLST_i = \frac{LST_i - LST_{\min}}{LST_{\max} - LST_{\min}} \quad (5)$$

where

$NLST_i$ normalized LST of the ith pixel,
LST_i initial LST of the ith pixel and
$LST_{\max}$ and   maximum and minimum LST value of the
$LST_{\min}$ reference LST image.

Table 2 Emissivity calculation from NDVI

NDVI	Land surface emissivity
NDVI < − 0.185	0.995
− 0.185 < NDVI < 0.157	0.970
0.157 < NDVI < 0.727	$1.0094 + 0.047 \times \ln(\text{NDVI})$
NDVI > 0.727	0.990

3.3 Calculation of UHIRI

Generally, the heat island strength indexes has been calculated by considering the higher LST pixels as urban and lower LST pixels as rural land cover. Since the barren land also shows higher LST during day time, it is important to distinguish the contribution of barren land and urban built-ups. Thus, the developed index named UHIRI is useful to understand the effect of urbanization on UHI intensity by considering the difference of LST for urban and natural land covers. This index determines the effect of built-up areas on LST as compared to the natural land covers present in the study area. Mean normalized LST of natural land covers (T_n) was calculated using Eq. (6).

$$T_n = \frac{\sum_i T_i \times P_i}{\sum_i P_i}; \quad i = 1, 2, 3 \tag{6}$$

where $i = 1, 2, 3$ refer to that of water, bare land and vegetated land respectively; T_i is the normalized LST of ith land cover and P_i is the percentage of ith land cover to the total study area. Further, computation of UHIRI was done using from Eq. (7),

$$UHIRI = \frac{T_b - T_n}{T_n} \tag{7}$$

where T_b is the mean normalized LST of urban land cover.

3.4 Computation of LCCI

In order to study the contribution of each LULC class on LST, statistics of normalized LST of each land cover, i.e. minimum LST, maximum LST, mean LST and SD on LST for each LULC, was determined for four different years. Since the different LULC types are present in different proportions, the LST statistics cannot describe the contribution of each LULC type on the whole study area. Thus, LCCI was computed which determines the contribution of each LULC type on the entire study area using Eq. (8) (Huang et al. 2019).

$$LCCI_i = (T_i - T_m) \times P_i \; ; \quad i = 1, 2, 3, 4 \tag{8}$$

where T_i is the mean normalized LST of ith LULC type and T_m is the mean LST of the entire study area. Therefore, $LCCI_i$ describes the quantitative contribution of each LULC type on the study area at a particular time period.

4 Results and discussion

4.1 Urbanization and its impact on LST

4.1.1 LULC classification and changes

Land cover classifications were carried out in Varanasi region for years of 1989, 1997, 2008 and 2018, and the images obtained are shown in Fig. 2. The accuracy assessment of the classification yielded overall accuracy of the classified images

Fig. 2 Land cover classification map of Varanasi representing major land covers, i.e. water, vegetation, bare land and urban for years 1989, 1997, 2008 and 2018
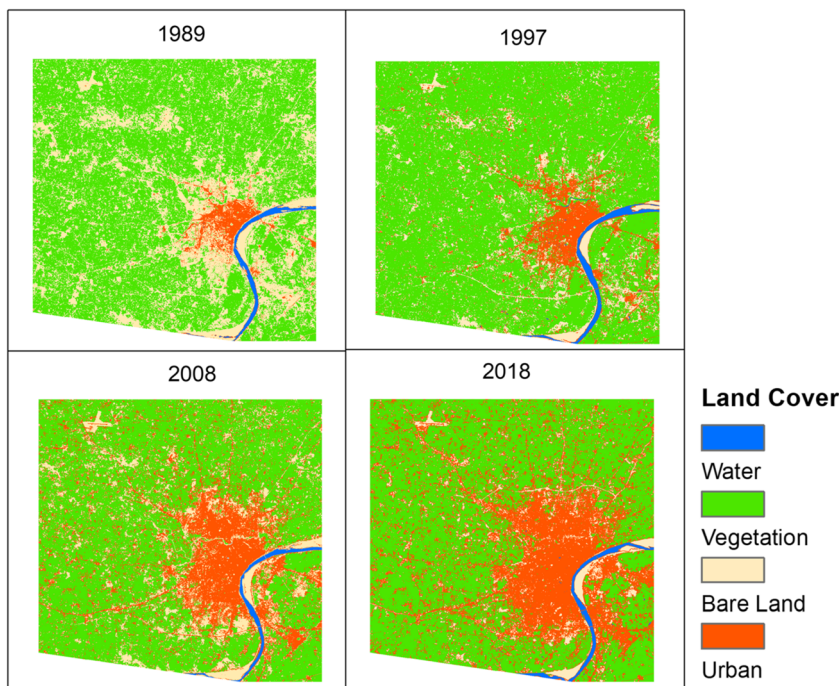
to be 95.2% for 1989, 93.7% for 1997, 94.3% for 2008 and 91.5 for 2018. The reasonable high accuracy of the classified images (above 90%) makes it suitable for analysis of urban expansion. The four major land covers were water, vegetation, bare land and built-ups. River Ganga was found to be the major source of water body in the city. The vegetated land covers constitute mainly the agricultural cropland. The bare land consists mainly of the fallow land and the dry river bed. Significant rise in the built-up land cover was observed from 1989 to 2018 indicating urban expansion.

Further, percentage of each LULC type to the total land cover (Total area = 866.87 km^2) was determined and shown in Fig. 3. The urban land cover was observed to increase in area by 62.07 km^2 from 1989 to 1997, 111.74 km^2 from 1997 to 2008 and 85.30 km^2 from 2008 to 2018. Therefore, 259.11 km^2 area of natural land cover was converted into urban built-ups from 1989 to 2018. Vegetation was observed to be the dominant among the natural land cover across the city. The contribution of bare soil percentage was high in 1989 (i.e. 32.52), and substantial decrease was found in 1997 (i.e. 11.88). The development of irrigation systems with advanced technology replaced various areas of bare land with agricultural vegetated areas. The Indo-Dutch Tubewell Project constructed various tubewells from year 1988 to 1993 to increase the area for irrigation for enhanced agricultural productivity (Alberts 1998). The Free Boring Scheme in Uttar Pradesh started in year 1984 and reached 2.5 million in year 2001 which was useful for providing enough water for irrigation purpose (Lata 2019). Thus, the vegetation contribution was lower, and bare land contribution was higher in year 1989 as compared to that in year 1997. The vegetation contribution was found to decrease from year 1997 to 2018. The urban expansion was the result of replacing bare land or vegetation with the urban built-ups.
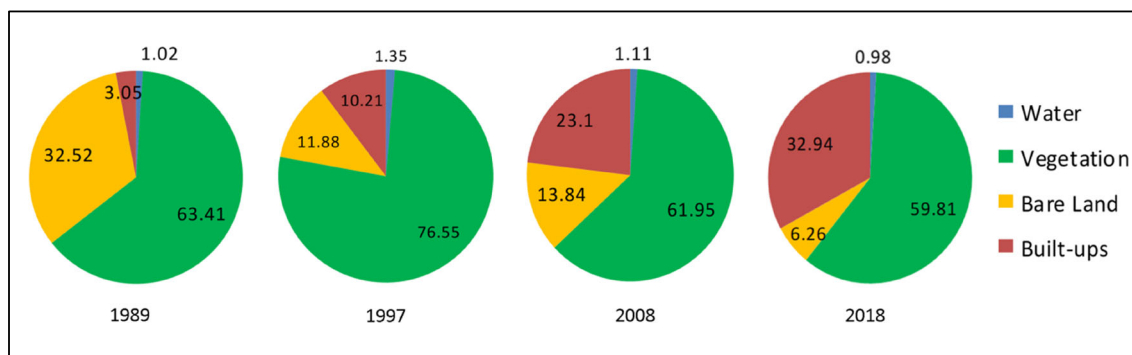
Urbanization mapping of Varanasi city from 1989 to 2018 is shown in Fig. 4 which was obtained from the classified map of Varanasi city. This reveals the areas that have experienced rapid urban growth in 29 years. From 1989 to 1997, urban expansion was observed in the northern and southern region from the centre of the city. Major urban expansion was observed from year 1997 to 2018 in all directions of the Varanasi city. The natural landscapes which are replaced by built-ups have direct influence on the LST of those areas.

4.1.2 Long-term study on LST and quantification of urban heat intensity using UHIRI

Figure 5 shows the normalized LST map for years 1989, 1997, 2008 and 2018. In order to study the LST dependence of each land cover, it is important to understand the thermal signature of each LULC type. Varanasi city is surrounded by agricultural region. Thus, the lower LST values surrounding the city were due to the vegetated areas or crops. The river Ganga at the eastern part of the city shows lower LST values, whereas the dry river bed results in very high LST as depicted from the four LST images. The high LST pixels across the city represent bare land. Therefore, the waterbody and vegetated land cover shows lower LST values, whereas bare land results in higher LST values as compared to the urban land cover. Mean normalized LST of entire study area were determined to be 0.33, 0.30, 0.31 and 0.29 for years 1989, 1997, 2008 and 2018, respectively. Normalized mean LST of 1989 shows higher value due to presence of more bare pixels. In spite of more urban pixels in 2018, mean normalized LST show lower value due to the presence of less number of bare pixels. The mean LST obtained includes contribution from all the land covers. Since bare pixels have significant influence on the LST, mean normalized LST cannot explain the influence of urbanization on LST in areas which has combined contribution of vegetation and bare land pixels in rural areas.

In order to determine the effect of urbanization of LST, a new index was proposed to quantify the urban heat intensity for the data used in the study named as UHIRI. This index was calculated using two major factors, i.e. the difference of urban LST with the rural LST and the proportion of urban land in a particular year. Figure 6 shows the value of UHIRI for the 4 years of study which determines the change in UHI intensity from year 1989 to 2018. The increase in UHIRI value with

Fig. 3 Percentage distribution of each LULC type, i.e. water, vegetation, bare land and built-ups in Varanasi city for years 1989, 1997, 2008 and 2018

Fig. 4 Urbanization mapping from 1989 to 2018 of Varanasi city. The change of natural land cover to urban land cover is shown for interval in years, i.e. 1989–1997, 1997–2008 and 2008–2018
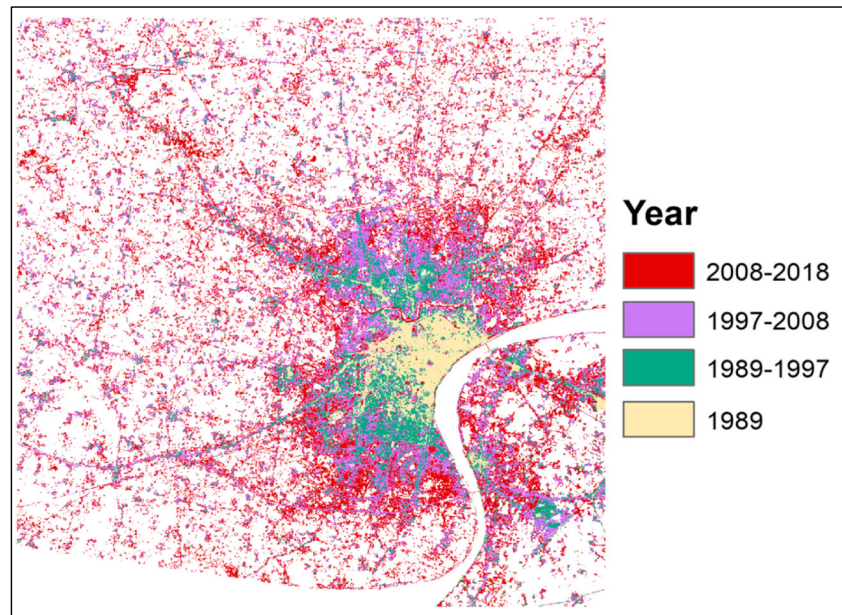
year clearly indicates the effect of urbanization on the LST of the city.

## 4.2 Effect of urban growth on LST based on land cover

4.2.1 LST dependence of each land cover

In order to further study the behaviour of LST with different LULC types, LST statistics of each land cover were obtained for the four different years and plotted as shown in Fig. 7. The figure shows the minimum, mean, SD and maximum LST values for each LULC types, and the mean LST of entire area was also shown in the figure. Various previous studies have obtained the behaviour of LST for different land covers and found that bare land shows higher LST, whereas water and vegetation areas show lower LST than urban areas during the day time (Amiri et al. 2009; Shastri et al. 2017). The LST behaviour of different land covers in this study for different years was found consistent with the previous studies. The higher LST values of bare land and built-ups as compared to the mean LST of entire area depict their positive contribution towards UHI. On the other hand, the lower LST values of

Fig. 5 Normalized LST map for years 1989, 1997, 2008 and 2018 of Varanasi city was obtained from Landsat images
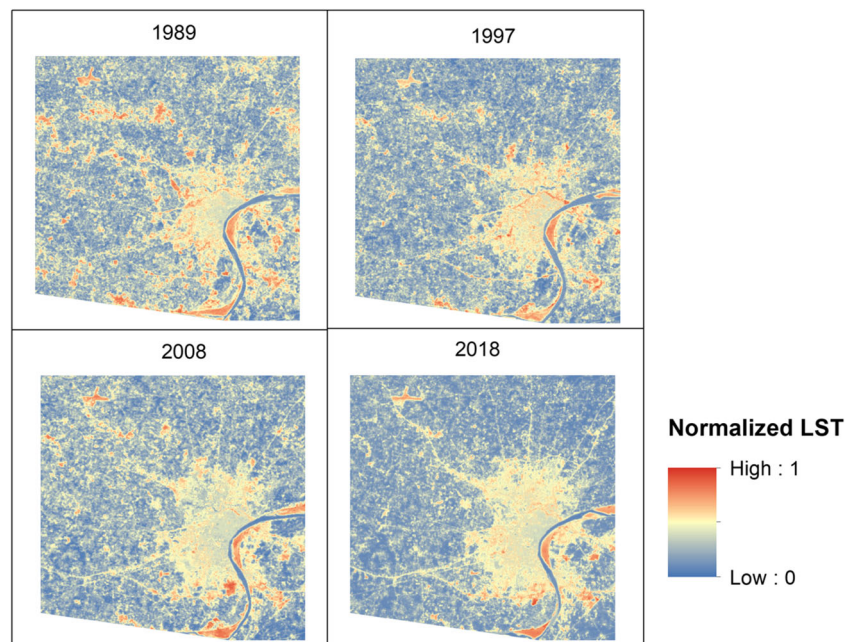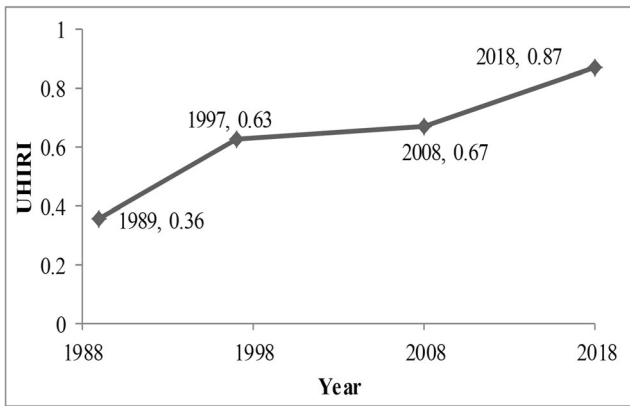
Fig. 6 The plot of Urban Heat Intensity Ratio Index (UHIRI) value for years 1989, 1997, 2008 and 2018 of Varanasi city

vegetation and waterbody in comparison with the mean LST of entire area depict their negative contribution towards UHI as observed in four different years of study. The mean normalized LST and SD for waterbody were found to show lower values as compared to the vegetated land cover in years 1989, 1997 and 2008, whereas both LULC classes show similar mean normalized LST values in 2018, but greater SD was observed for waterbody. Thus, water pixels show lesser

contribution towards lowering UHI in 2018. The SD of bare land and built-ups were found greater than water and vegetation. Soil moisture content of the bare land may vary resulting in greater variation of LST values. The urban built-ups are made up of different materials with varying heat capacity resulting in greater variation in LST values. Thus, the LST statistics determines the contribution of each land cover towards UHI.

4.2.2 Quantifying the contribution of LULC types on LST

The land cover was observed to change from the year 1989 to 2018 due to urbanization which has the capability to modify the thermal environment. The area occupied by each land cover was observed to change with time. The contribution of each land cover on UHI also depends on the proportion of the LULC type present in the region. Thus, the quantification of contribution of each LULC class requires contribution of both LST and the proportion of that LULC class present in the study area. Therefore, LCCI was calculated for each LULC type for the years 1989, 1997, 2008 and 2018 to quantify the contribution of each land cover and is shown in Table 3. The LULC class with high LST, i.e. bare land and built-ups, shows
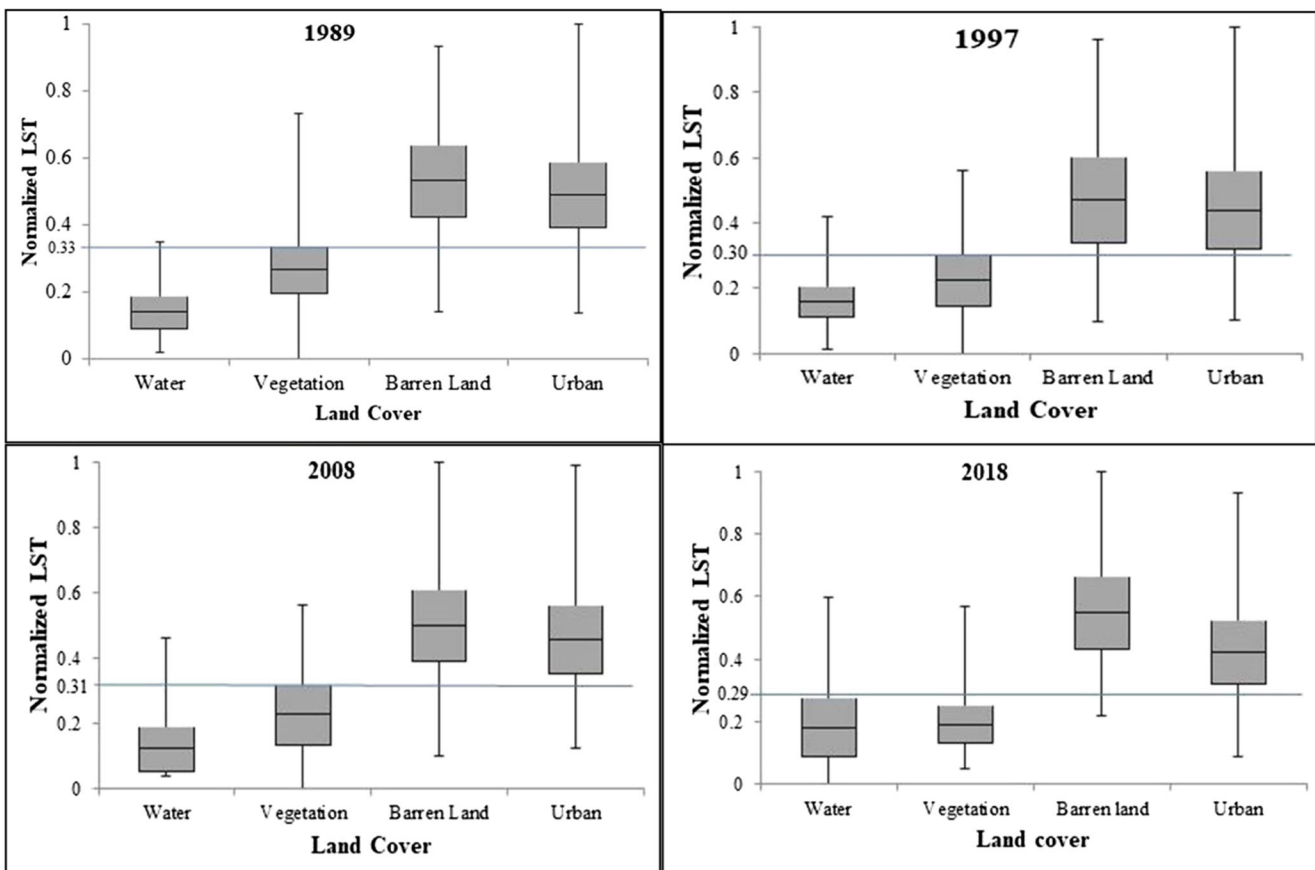
Fig. 7 Normalized LST statistics of water, vegetation, bare land and urban land covers for years 1989, 1997, 2008 and 2018 of Varanasi city. Each bar represents the mean ± SD of normalized LST for each land cover. The horizontal line depicts the mean normalized LST for that year

Table 3 Land cover contribution index (LCCI) of each land cover, i.e. water, vegetation, bare land and urban for years 1989, 1997, 2008 and 2018

Land cover	1989	1997	2008	2018
Water	− 0.19	− 0.19	− 0.21	− 0.11
Vegetation	− 3.99	− 5.28	− 5.23	− 5.83
Bare land	6.57	2.02	2.63	1.63
Urban	0.49	1.43	3.40	4.37

positive value of LCCI, and those LULC classes with low LST, i.e. vegetation and waterbody, show negative value of LCCI. The magnitude of the LCCI depicts the quantitative contribution of each LULC type on LST. The LCCI values for built ups from 1989 to 2018 were plotted and shown in Fig. 8. The significant increase in LCCI values for built-ups indicates quantitative increase in contribution of built-up on UHI with urban expansion. The LCCI value can distinguish the contribution of bare land and built-ups towards increase in LST which was not possible from the LST statistics. Hence, the LCCI was found useful for quantification of contribution of each LULC type on UHI.

The behaviour of UHIRI can also be discussed using the LCCI of each land cover. The LCCI magnitude was found to decrease for bare land and increase for vegetation which resulted in lowering of mean LST of natural land cover. The temperature difference of urban and LST increases, and its combination with the increased built-up land cover shows sharp increase in UHIRI value from 1989 to 1997 (0.36 to 0.63). From 1997 to 2008, the slight decrease in vegetation contribution and increase in bare land contribution result in increased mean LST of natural land cover which leads to decrease in the urban and rural temperature difference. By combining this with the increased built-up contribution shows

increase in UHIRI value but with a lower magnitude (0.63 to 0.67). Further, the UHIRI value from 2008 to 2018 shows sharp increase due to increased contribution of vegetation and decreased contribution of bare land. The UHIRI value includes both the contribution of temperature difference from built-up and natural land cover as well as proportion of built-up land in the study areas. Therefore, this index has the potential to explain the effect of urbanization on LST in areas with greater heterogeneity in LULC types.

4.2.3 LULC change and its effect on LST

Changes in LULC were observed from 1989 to 2018 which has great impact on the LST of the areas within study. It is important to analyse the type of LULC changes that had occurred, i.e. natural land cover to other type of natural land cover or natural land cover to urban land cover. The classified maps of 1989 and 2018 were used to determine the pixels where LULC changes had occurred and shown in Fig. 9. The bare land and vegetation among the natural land covers that have been replaced by artificial built-up surfaces as a consequence of urbanization were shown in the change map. Other changes in the map reveal areas where natural land cover was changed by other type of natural land cover which mainly consists of conversion from bare land to vegetation or vegetation to bare land. Therefore, the pixels that have been converted due to urbanization can be clearly identified from the change map.

It is important to study the impact on LST due to increased urbanization. The vegetated pixels show lower LST, and the bare land pixels show higher LST as compared to the urban pixels. Thus, LST change from bare land to urban and vegetated pixels to urban may show different behaviour. The mean change in normalized LST was calculated for the pixels being converted from bare land to urban and vegetation to urban and

Fig. 8 The plot of land cover contribution index (LCCI) for urban land cover from 1989 to 2018 for Varanasi city
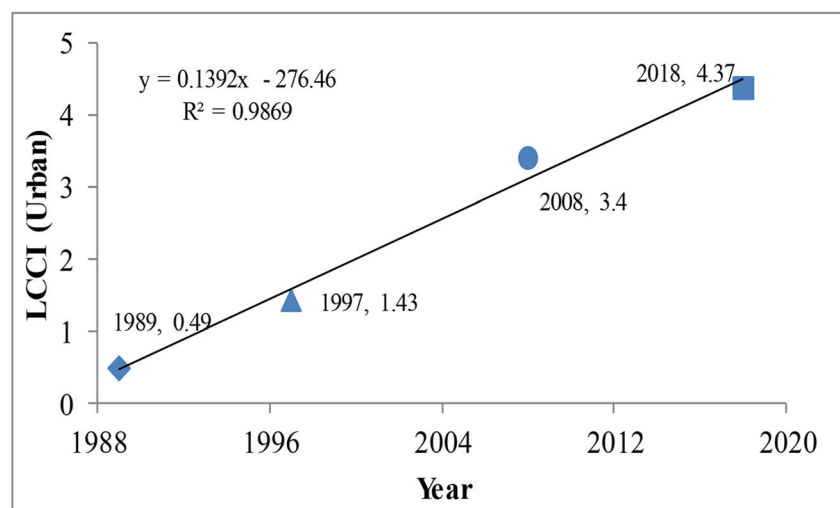
Fig. 9 Land cover change map of Varanasi city for the period 1989 to 2018. The change map highlights the pixels converted from vegetation or bare land to urban land cover
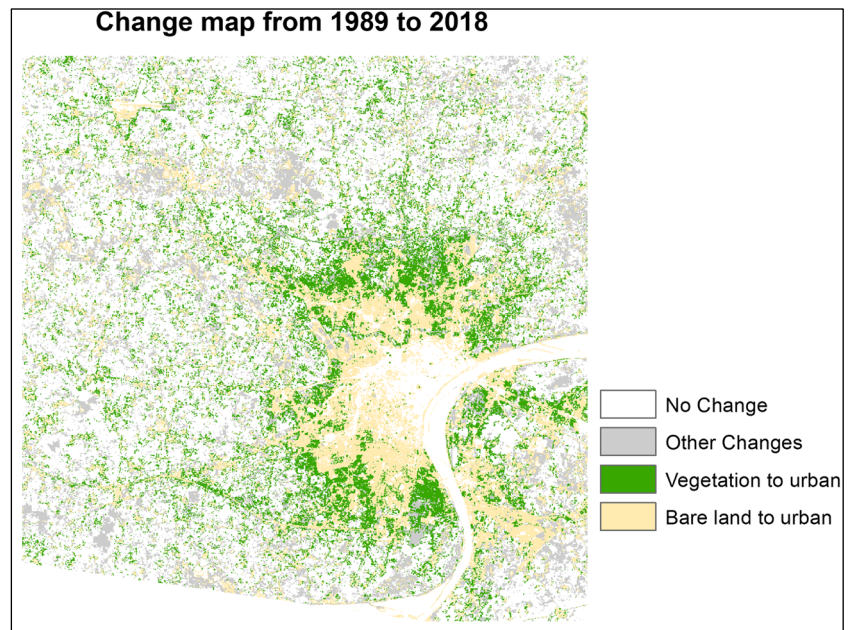
plotted as shown in Fig. 10. Bare land to urban pixels was observed to show negative value with lower magnitude for change in LST which reveals small decrease in LST with this type of urbanization. Vegetation to urban pixels was observed to show positive value with higher magnitude of change in LST which reveals significant increase in LST. Hence, urbanization on bare land has very less effect on LST, whereas that on vegetated land provides remarkable heating effect. Therefore, replacement of vegetation with urban land cover has severe impact on increasing the intensity of UHI effect.
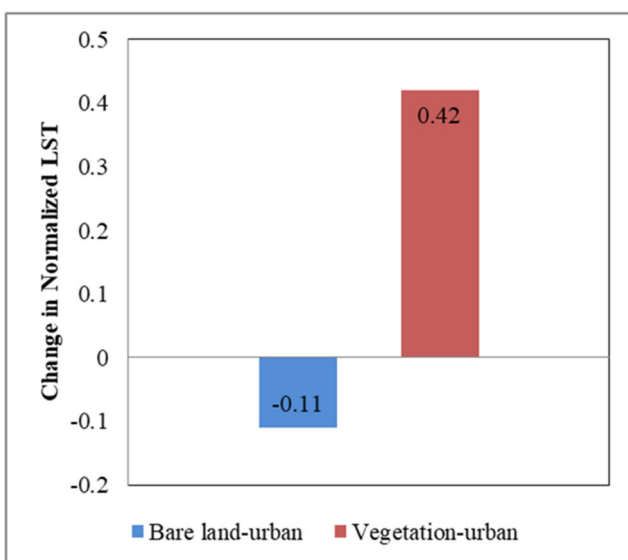
Fig. 10 Mean change in normalized LST for pixels converted from bare land or vegetation to urban land cover in Varanasi city

5 Conclusion

In the present study, the effect on LST due to the increase in urbanization was analysed in Varanasi city of India between years 1989 and 2018 using Landsat satellite images. The classified maps of Varanasi city were obtained for years 1989, 1997, 2008 and 2018 and found that the area of 259.11 km^2 of natural land cover was converted into urban built-ups between years 1989 and 2018. Thus, a new index named UHIRI was proposed to quantify the urban heat intensity with increasing urbanization between years 1989 and 2018 in the Varanasi city. UHIRI value was found to increase from 0.36 in year 1989 to 0.87 in year 2018 which reveals that urbanization has significant impact on urban temperatures.

In order to study the behaviour of LST with different LULC types, LST statistics of each land cover were obtained for the four different years, i.e. 1989, 1997, 2008 and 2018, and found that the bare land and built-up land covers show higher LST values as compared to the mean LST of entire area revealing positive contribution towards UHI. The vegetation and waterbody was found to show lower LST values as compared to the mean LST of entire area depicting their negative contribution towards UHI. Further, contribution of each land cover towards raising or lowering of LST was determined using LCCI for years 1989, 1997, 2008 and 2018 to analyse the variation in contribution of each land cover towards LST with change in LULC. The water and vegetation LULC types were found to show negative value of LCCI, whereas the bare land and built-ups showed positive value of LCCI. The LCCI value for urban land cover was found to increase from 0.49 in year 1989 to 4.37 in year 2018 which reveals the significant

increase in contribution of urban land cover towards LST. The LCCI value for each land cover was used to understand the behaviour of UHIRI value. The UHIRI value includes both the contribution of temperature difference from built-up and natural land cover as well as proportion of built-up land in the study areas. Hence, this index has the potential to explain the effect of urbanization on LST in areas with greater heterogeneity in LULC types.

The urbanization occurs with two types of LULC changes, i.e. bare land to built-ups or vegetation to built-ups. The mean difference in normalized LST was calculated for the pixels being converted from bare land to urban and vegetation to urban from years 1989 to 2018. Bare land to urban pixels was observed to show small decrease in normalized LST, whereas vegetation to urban pixels showed significant increase in normalized LST. Therefore, replacement of vegetation with urban land cover has severe impact on increasing the intensity of UHI effect.

Therefore, this analysis discusses about quantification of the UHI effect with increasing urbanization and also the contribution of each land cover towards UHI. Further studies can be performed to study the effect on night LST with changing LULC types and contribution of each land cover on night LST with increasing urbanization.

Author contribution Ruchi Bala: conceptualization, data curation, formal analysis, investigation, methodology, software handling, validation, writing of original draft, writing of review and editing. Rajendra Prasad: resources, supervision, writing of review and editing. Vijay Pratap Yadav: data curation, investigation, software handling, writing of review and editing.

Availability of data and material The Landsat satellite data was used for the study and downloaded from the website of Earth Explorer that was freely available for users.

Code availability Software: Envi 5.1, Matlab, QGIS.

Declarations

Ethics approval Not applicable.

Consent to participate Not applicable.

Consent to publication Not applicable.

Conflict of interest The authors declare no competing interests.

References

Alberts JH (1998). Public tubewell irrigation in Uttar Pradesh, India: a case study of the indo-Dutch tubewell project. International Institute for Land Reclamation and Improvement

Amiri R, Weng Q, Alimohammadi A, Alavipanah SK (2009) Spatial–temporal dynamics of land surface temperature in relation to fractional vegetation cover and land use/cover in the Tabriz urban area, Iran. Remote Sens Environ 113(12):2606–2617

Aniello C, Morgan K, Busbey A, Newland L (1995) Mapping micro-urban heat islands using Landsat TM and a GIS. Comput Geosci 21(8):965–969

Barsi JA, Schott JR, Palluconi FD, Hook SJ (2005) Validation of a web-based atmospheric correction tool for single thermal band instruments. In: Earth observing systems X (Vol. 5882, p. 58820E). International Society for Optics and Photonics, Bellingham, Washington

Chen X-L, Zhao H-M, Li P-X, Yin Z-Y (2006) Remote sensing image-based analysis of the relationship between urban heat island and land use/cover changes. Remote Sens Environ 104(2):133–146

Grigoraş G, Uriţescu B (2019) Land use/land cover changes dynamics and their effects on surface urban Heat Island in Bucharest, Romania. Int J Appl Earth Obs Geoinf 80:115–126

Huang C, Thomas N, Goward SN, Masek JG, Zhu Z, Townshend JR, Vogelmann JE (2010) Automated masking of cloud and cloud shadow for forest change analysis using Landsat images. Int J Remote Sens 31(20):5449–5464

Huang Q, Huang J, Yang X, Fang C, Liang Y (2019) Quantifying the seasonal contribution of coupling urban land use types on urban Heat Island using land contribution index: a case study in Wuhan, China. Sustain Cities Soc 44:666–675

Jha DK, Harshwardhan R, Tripathi VK (2019) Geographical zones of Varanasi City: past to present. National Geographical Journal of India 65(1):46–55

Kato S, Yamaguchi Y (2005) Analysis of urban heat-island effect using ASTER and ETM+ data: separation of anthropogenic heat discharge and natural heat radiation from sensible heat flux. Remote Sens Environ 99(1–2):44–54

Keeratikasikorn C, Bonafoni S (2018) Urban heat island analysis over the land use zoning plan of Bangkok by means of Landsat 8 imagery. Remote Sens 10(3):440

Lata S (2019) Irrigation water management for agricultural development in Uttar Pradesh. Springer International Publishing, India

Li H, Zhou Y, Li X, Meng L, Wang X, Wu S, Sodoudi S (2018) A new method to quantify surface urban heat island intensity. Sci Total Environ 624:262–272

Mathew A, Khandelwal S, Kaul N (2016) Spatial and temporal variations of urban heat island effect and the effect of percentage impervious surface area and elevation on land surface temperature: study of Chandigarh city, India. Sustain Cities Soc 26:264–277

Mathew A, Khandelwal S, Kaul N (2018) Investigating spatio-temporal surface urban heat island growth over Jaipur city using geospatial techniques. Sustain Cities Soc 40:484–500

Meng Q, Zhang L, Sun Z, Meng F, Wang L, Sun Y (2018) Characterizing spatial and temporal trends of surface urban heat island effect in an urban main built-up area: a 12-year case study in Beijing, China. Remote Sens Environ 204:826–837

Qiu S, Zhu Z, Woodcock CE (2020) Cirrus clouds that adversely affect Landsat 8 images: what are they and how to detect them? Remote Sens Environ 246:111884

Rao PK (1972) Remote sensing of urban heat islands from an environmental satellite. Bull Am Meteorol Soc 53:647–648

Sarrat C, Lemonsu A, Masson V, Guedalia D (2006) Impact of urban heat island on regional atmospheric pollution. Atmos Environ 40:1743–1758

Shafizadeh-Moghadam H, Weng Q, Liu H, Valavi R (2020) Modeling the spatial variation of urban land surface temperature in relation to environmental and anthropogenic factors: a case study of Tehran, Iran. GIScience & Remote Sensing 57(4):483–496

Shastri H, Barik B, Ghosh S, Venkataraman C, Sadavarte P (2017) Flip flop of day-night and summer-winter surface urban heat island intensity in India. Sci Rep 7:40178

Shirani-Bidabadi N, Nasrabadi T, Faryadi S, Larijani A, Roodposhti MS (2019) Evaluating the spatial distribution and the intensity of urban heat island using remote sensing, case study of Isfahan city in Iran. Sustain Cities Soc 45:686–692

Singh A (1989) Review article digital change detection techniques using remotely-sensed data. Int J Remote Sens 10(6):989–1003

Streutker DR (2003) Satellite-measured growth of the urban heat island of Houston, Texas. Remote Sens Environ 85:282–289

Sultana S, Satyanarayana ANV (2018) Urban heat island intensity during winter over metropolitan cities of India using remote-sensing techniques: impact of urbanization. Int J Remote Sens 39(20):6692–6730

Taha H (1997) Urban climates and heat islands: albedo: evapotranspiration and anthropogenic heat. Energy and Buildings 25:99–103

Tiangco M, Lagmay AMF, Argete J (2008) ASTER-based study of the night-time urban heat island effect in metro Manila. Int J Remote Sens 29(10):2799–2818

Tran H, Uchihama D, Ochi S, Yasuoka Y (2006) Assessment with satellite data of the urban heat island effects in Asian mega cities. Int J Appl Earth Obs Geoinf 8:34–48

United Nation (2015) World urbanization prospects: the 2014 revision, New York

Van de Griend AA, Owe M (1993) On the relationship between thermal emissivity and the normalized difference vegetation index for natural surfaces. Int J Remote Sens 14:1119–1131

Voogt JA, Oke TR (2003) Thermal remote sensing of urban area. Remote Sens Environ 86:370–384

Yuan F, Bauer ME (2007) Comparison of impervious surface area and normalized difference vegetation index as indicators of surface urban heat island effects in Landsat imagery. Remote Sens Environ 106(3):375–386

Zhang J, Wang Y (2008) Study of the relationships between the spatial extent of surface urban heat islands and urban characteristic factors based on Landsat ETM+ data. Sensors 8(11):7453–7468

Zhang K, Wang R, Shen C, Da L (2010) Temporal and spatial characteristics of the urban heat island during rapid urbanization in Shanghai, China. Environ Monit Assess 169:101–112